



OPEN

Metallosalen modified carbon nitride a versatile and reusable catalyst for environmentally friendly aldehyde oxidation

Reza Eskandari Sedighi¹, Mahdi Behzad¹✉ & Najmedin Azizi²✉

The development of environmentally friendly catalysts for organic transformations is of great importance in the field of green chemistry. Aldehyde oxidation reactions play a crucial role in various industrial processes, including the synthesis of pharmaceuticals, agrochemicals, and fine chemicals. This paper presents the synthesis and evaluation of a new metallosalen carbon nitride catalyst named Co(salen)@g-C₃N₄. The catalyst was prepared by doping salicylaldehyde onto carbon nitride, and subsequently, incorporating cobalt through Schiff base chemistry. The Co(salen)@g-C₃N₄ catalyst was characterized using various spectroscopic techniques including Scanning Electron Microscopy (SEM), X-ray Diffraction (XRD), Infrared Spectroscopy (IR), and Thermogravimetric Analysis (TGA). Furthermore, after modification with salicylaldehyde, the carbon nitride component of the catalyst exhibited remarkable yields (74–98%) in oxidizing various aldehyde derivatives (20 examples) to benzoic acid. This oxidation reaction was carried out under mild conditions and resulted in short reaction times (120–300 min). Importantly, the catalyst demonstrated recyclability, as it could be reused for five consecutive runs without any loss of activity. The reusable nature of the catalyst, coupled with its excellent yields in oxidation reactions, makes it a promising and sustainable option for future applications.

Keywords Carbon nitride, Metallosalen, Aldehyde, Green chemistry, Oxidation, Hydrogen peroxide

Selective oxidation of aldehydes to acids is one of the most important reactions in the chemical industry¹. Among these reactions, the oxidation of benzyl alcohol to benzaldehyde and its conversion into valuable products in the fragrance, dye, pharmaceutical, and chemical industries make it a significant chemical process^{2–4}. In recent decades, the development of processes utilizing safe and economically feasible oxidants has attracted considerable attention from researchers^{5–8}. The oxidation of aldehydes using molecular oxygen (O₂) as the oxidizing agent has garnered significant research interest due to its environmentally friendly nature and low cost^{9–12}. Furthermore, the selection of a desirable catalyst and the avoidance of hazardous solvents are also crucial aspects of these processes^{13–17}. Heterogeneous catalysts present notable advantages over homogeneous catalysts, due to their easy separation from the reaction medium and the possibility of catalyst reuse^{18–20}.

In recent decades, Schiff bases have played a key role as chelating ligands in coordination chemistry of transition metals and main group metals²¹. These ligands can easily form stable complexes with a variety of metal ions^{22,23}. Transition metal complexes with oxygen- and nitrogen-donor Schiff base ligands have special significance due to their ability to adopt diverse configurations, structural flexibility, and sensitivity to molecular environments^{24,25}. Metal complexes formed by Schiff base ligands that have both hard donor atoms such as oxygen and nitrogen and soft donor atoms such as sulfur often exhibit interesting physical and chemical properties^{26,27}. Schiff bases have diverse applications in various fields such as industry, medicine, and chemical synthesis^{28,29}. Their properties include antimicrobial and antibacterial effects, anticancer, antioxidant, and catalytic properties, as well as applications in organic synthesis, photochromism^{30–32}, and other applications, which have attracted the attention of researchers to prepare various types of Schiff bases through bifunctional reactions^{33–35}.

Graphitic carbon nitride (g-C₃N₄) is a carbon-based material that has gained attention in various research fields^{36–40}, including catalysis, energy storage, optoelectronics, and environmental applications^{41–44}. It offers high chemical stability and a tunable bandgap, making it suitable for optoelectronics and photocatalysis^{45–48}. In

¹Faculty of Chemistry, Semnan University, Semnan, Iran. ²Chemistry and Chemical Engineering Research Center of Iran, P.O. Box 14335-186, Tehran, Iran. ✉email: mbehzad@semnan.ac.ir; azizi@cerci.ac.ir

photocatalysis, it has shown excellent performance in water splitting, pollutant degradation, and carbon dioxide reduction^{49,50}. Carbon nitride also has interesting electronic properties as a semiconductor, which can be modified for enhanced charge transport in electronic devices like sensors and transistors^{51–53}.

Our continuous interest in carbon nitride chemistry and our ongoing research aims to explore new synthetic strategies, optimize catalytic performance, and expand the scope of carbon nitride-based catalysts in various organic transformations^{54–56}. Considering the presence of the nitrogen functional group on carbon nitride, this inexpensive platform can be used as a support and Schiff base agent. In this article, the advantage of carbon nitride was utilized for the preparation of Schiff base complexes involving copper, cobalt, and manganese. Carbon nitride was used as a support material as well as the Schiff base agent. The nitrogen atoms in carbon nitride were reacted with salicylaldehyde to provide a stable environment for the formation of Schiff base complexes. This approach allows for the immobilization of metal ions on carbon nitride, leading to the synthesis of supported Schiff base catalysts.

Experimental

Preparation of g-C₃N₄

The synthesis of bulk g-C₃N₄ involved a direct heating method using melamine in air, following the procedure outlined in the previous paper²³. 20 g (158 mmol) of melamine powder was placed into a covered 50 mL alumina crucible and was subjected to gradual heating in a muffle furnace. The temperature was increased at a rate of 5 °C per minute until reaching a final temperature of 550 °C and maintained at 550 °C for 4 h. After the reaction time, the crucible was allowed to cool down naturally to room temperature. A light-yellow powder, which corresponds to the synthesized bulk g-C₃N₄, was obtained and collected from the crucible. The g-C₃N₄ nanosheets were prepared through thermal exfoliation. The 5 g of bulk g-C₃N₄ was placed into an uncovered crucible. The crucible with the bulk g-C₃N₄ was subjected to heat treatment in a furnace at a temperature of 550 °C for 3 h. After the heat treatment, a white powder, consisting of g-C₃N₄ nanosheets, was obtained.

Preparation of Co(salen)@g-C₃N₄

1 g of g-C₃N₄ was added to a dry ethanol solution (50 mL) and the mixture was an ultrasound with ultrasonic probe for 10 min to ensure proper dispersion of g-C₃N₄ in ethanol. To the g-C₃N₄ suspension, 0.5 g (4 mmol) of salicylaldehyde was added. The resulting suspension was refluxed for 24 h with constant stirring. The solution was allowed to cool to room temperature. It was then washed twice with 15 mL portions of ethanol. 1.0 g of salen@g-C₃N₄ was dispersed in 50 mL of dry ethanol and 0.5 g (4 mmol) of cobalt(II) chloride was added. The resulting solution was stirred at reflux for 8 h. After the refluxing period, the solid product was washed twice with 15 mL portions of ethanol and dried (Fig. 1).

Experimental procedure

In a test tube equipped with a magnetic stirring bar and septum was charged with Co(salen)@g-C₃N₄ (30 mg), aldehydes (1 mmol), and H₂O₂ (3 mmol). The mixture was heated at 60 °C with stirring until the reaction was complete, followed by cooling to room temperature. Water (10 mL) was added to quench the reaction, and the resulting mixture was then extracted with ethyl acetate (10 mL). The organic layer was dried using MgSO₄, and the solvent was evaporated under vacuum. In most cases, the reaction products were obtained in high purity and did not require additional purification methods. ¹H and ¹³C NMR analysis and comparison of the melting points with literature values confirmed the identity of the compounds. In a few cases, crude products were further purified using silica column chromatography with ethyl acetate and petroleum ether as eluents.

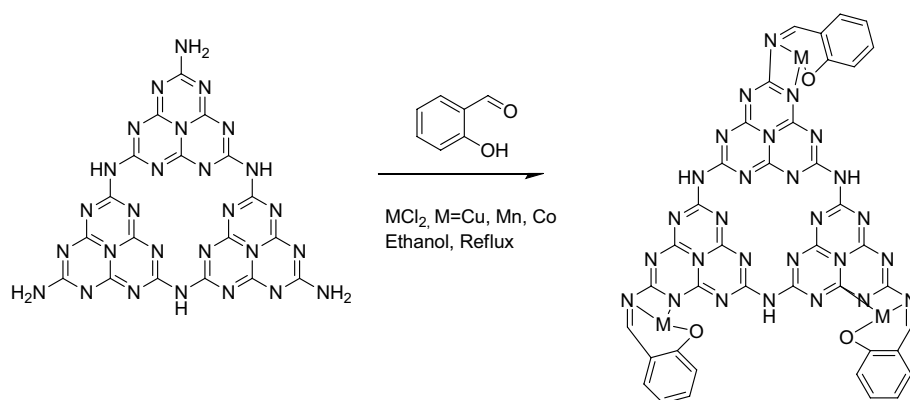


Figure 1. Preparation of the Co(salen)@g-C₃N₄ catalysts.

Results and discussion

The characterization of $\text{Co}(\text{salen})@g\text{-C}_3\text{N}_4$ crystalline structures was carried out using powder PXRD (Fig. 2). The PXRD patterns¹² of $\text{Co}(\text{salen})@g\text{-C}_3\text{N}_4$ showed two major peaks of diffraction at approximately 27.7° and 13.1° , as depicted in Fig. 1. The peak at around 27.7° was identified as the (002) plane, which arises from the interplanar stacking of aromatic systems.

A slight decrease in the peak intensity was observed after the incorporation of the Co complex compared to that of unmodified carbon nitride. However, it was observed that the functionalization of $g\text{-C}_3\text{N}_4$ with the Co complex did not alter the crystalline structure as with pure $g\text{-C}_3\text{N}_4$ (Figure S1 in Supporting Information).

The SEM images of $\text{Co}(\text{salen})@g\text{-C}_3\text{N}_4$ at different magnitudes were performed to support the structural and spectroscopic features, and get more information about the catalyst, and results are shown in Fig. 3. $g\text{-C}_3\text{N}_4$ was produced through direct calcination of melamine and showed a two-dimensional (2D) structure consisting of stacked thin sheets with wrinkles and irregular shapes. These sheets have noticeable micro-holes on their surfaces, adding to the material's unique characteristics. The 2D structure of $g\text{-C}_3\text{N}_4$ did not change after incorporation of $\text{Co}(\text{salen})$ on the surface of carbon nitride (Figure S2 in Supporting Information).

The EDX spectroscopy image of $\text{Co}(\text{salen})@g\text{-C}_3\text{N}_4$ is shown in Fig. 4. The EDS spectrum provided in Fig. 4 confirms the presence of the chemical compound CoCl_2 in the $g\text{-C}_3\text{N}_4$ catalyst. The spectrum shows the appearance of elements related to Co (cobalt), Cl (chlorine), O (oxygen), N (nitrogen), and C (carbon). This provides evidence of the presence of these elements and their compounds on the surface of $\text{Co}(\text{salen})@g\text{-C}_3\text{N}_4$ catalyst.

The FTIR (Fig. 5) confirms the functionalization of graphitic carbon nitride surface and several characteristic absorption bands appeared in the FTIR spectrum. FTIR spectra of $g\text{-C}_3\text{N}_4$, showed typical C-N heterocycle stretches at 1251 , 1325 , 1450 , 1578 , and 1635 cm^{-1} , as well as the characteristic breathing mode of triazine units at 889 cm^{-1} . The broad absorption bands at 3156 cm^{-1} correspond to the stretching vibrations of hydroxyl bonds associated with adsorbed water in the crystal lattice of carbon nitride. These hydroxyl bonds are physically and chemically attached to the crystalline structure of carbon nitride and manifest as a broad peak in the FTIR spectrum. Furthermore, a narrow peak at 619 cm^{-1} that is due to the intrinsic Co-O stretching vibration indicates the presence of Co in the catalyst.

To assess the thermal stability of the catalyst, thermogravimetric analysis (TGA and TG) was conducted under an air atmosphere, ranging from 50 to 800°C . During the TGA, the sample's weight change was monitored as it was subjected to increasing temperatures. This analysis provides valuable information about the decomposition and thermal behavior of the carbon nitride polymer, allowing for a better understanding of its stability and potential applications (Fig. 6a,b). According to the observations presented in Fig. 6a, the initial mass loss occurring below 200°C is primarily attributed to the evaporation of adsorbed water or other volatile impurities present on the surface of the sample. As the temperature increases, the heating process leads to the decomposition of the applied salicylaldehyde and $g\text{-C}_3\text{N}_4$. This decomposition results in the chemical conversion of the salicylaldehyde into carbon-containing gases and $g\text{-C}_3\text{N}_4$ into nitrogen and carbon-containing gases. The decomposition of salicylaldehyde initiates at 200°C and is completed by 350°C . The main region of weight loss occurs between 350 and 550°C , which corresponds to the decomposition of carbon nitride. At temperatures exceeding 600°C , a residual weight of 1% is observed, which is attributed to the presence of cobalt oxide content in the catalyst.

After the preparation and characterization of the $\text{Co}(\text{salen})@g\text{-C}_3\text{N}_4$ catalyst, its catalytic performance for the oxidation of benzaldehyde and its derivatives was investigated. The model reaction chosen for this study was the oxidation of benzaldehyde using H_2O_2 . The goal was to optimize the yields and reaction times by varying the amount of catalyst, oxidation conditions, and temperature. The results of these optimization experiments are presented in Table 1. In the control reactions without the catalyst (Table 1, entry 1), the oxidation reaction of benzaldehyde with H_2O_2 did not proceed readily, resulting in low product yields. However, when metal-containing $\text{M}(\text{salen})@g\text{-C}_3\text{N}_4$ catalysts were introduced, the oxidation reaction was promptly initiated. As shown in Table 1, the catalytic activity of the $\text{M}(\text{salen})@g\text{-C}_3\text{N}_4$ catalysts followed the trend of

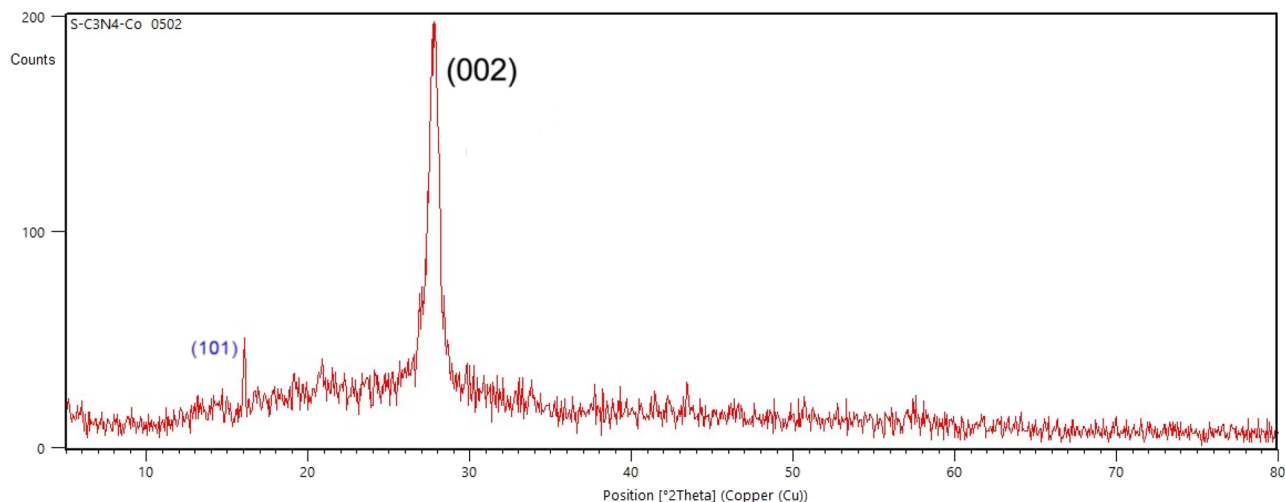


Figure 2. PXRD pattern of $\text{Co}(\text{salen})@g\text{-C}_3\text{N}_4$.

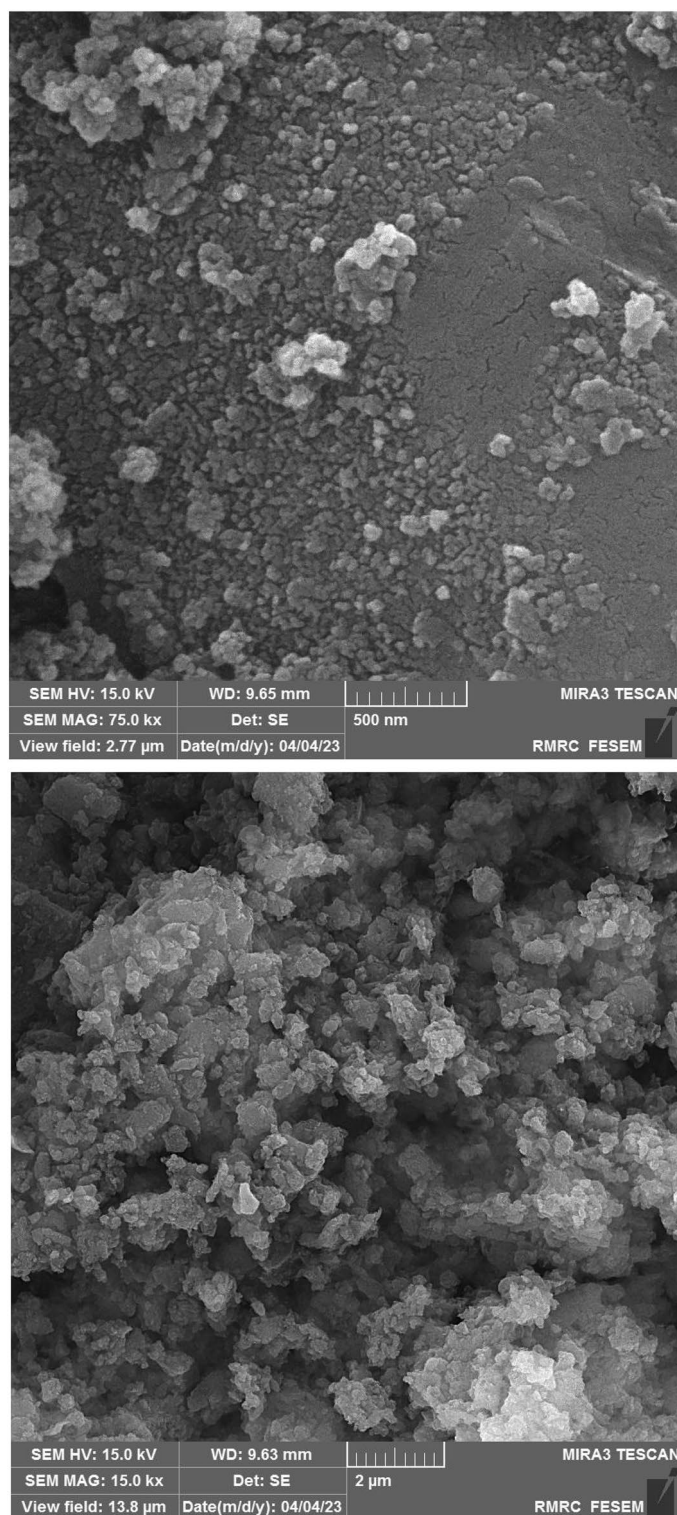


Figure 3. SEM image of Co(salen)@g-C₃N₄.

Co(salen)@g-C₃N₄ > Mn(salen)@g-C₃N₄ > Cu(salen)@g-C₃N₄, with decreasing activity observed (Table 1, entries 2–4). The highest yield (98%) of the desired benzoic acid **2a** was achieved after 20 h of reaction at room temperature, using 3 equivalents of H₂O₂ under solvent-free conditions (entry 4). It should be noted that reducing the amount of H₂O₂ resulted in a decrease in yield (Table 1, entries 5–8). The next step involved investigating the influence of the amount of Co(salen)@g-C₃N₄ catalyst in the oxidation system. It was observed that increasing the amount of catalyst had a significant impact on the oxidation efficiency. As the amount of catalyst increased, the oxidation yields improved. Specifically, when the catalyst amount was 5 mg, 10 mg, 20 mg, and 40 mg, the

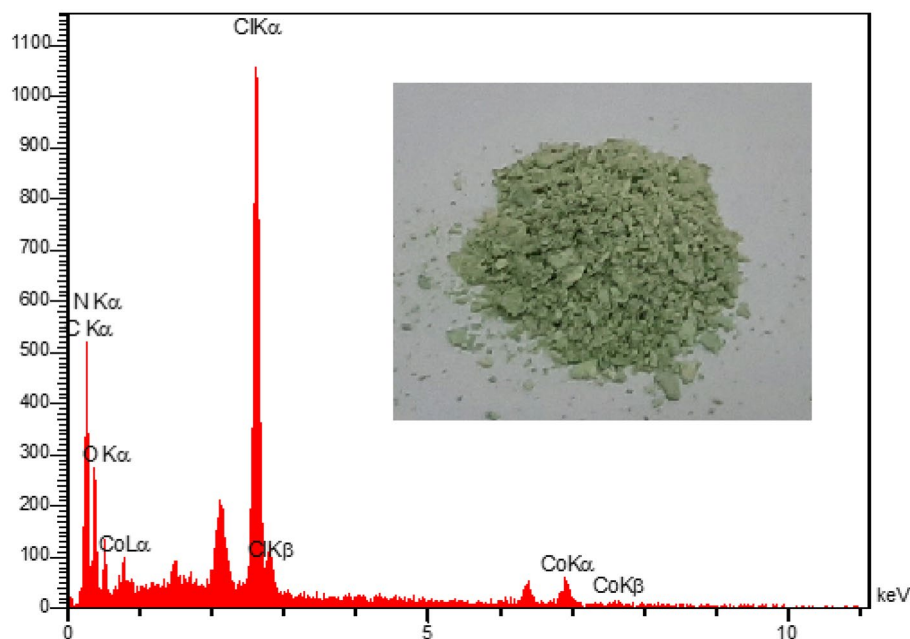


Figure 4. EDX pattern of Co(salen)@g-C₃N₄.

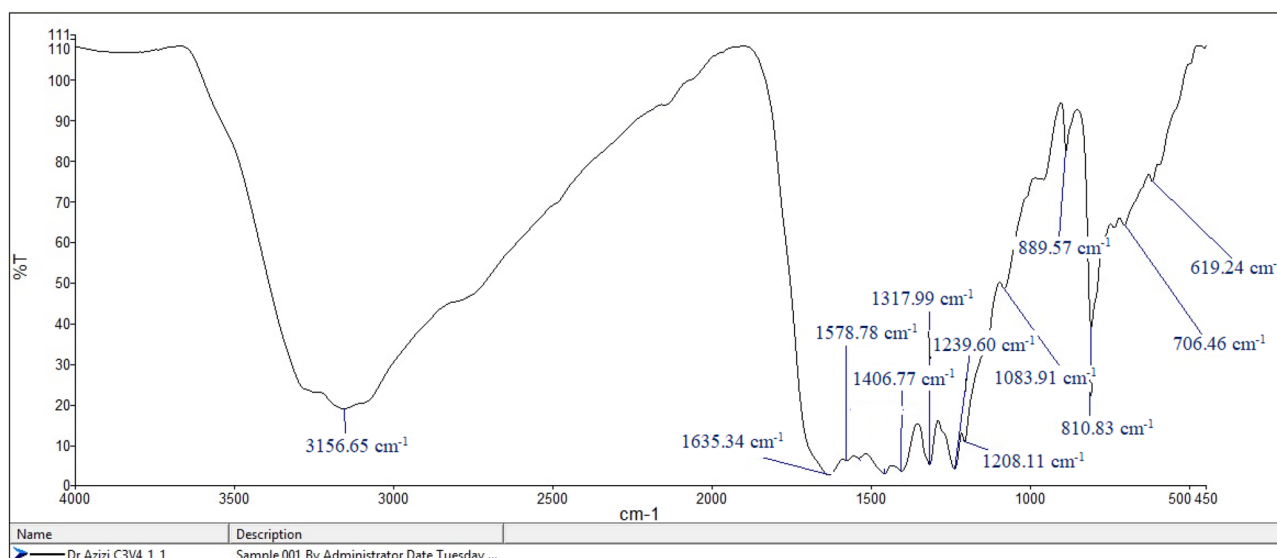


Figure 5. FTIR spectra of Co(salen)@g-C₃N₄.

oxidation yields were 51%, 68%, 81%, and 98%, respectively (Table 1, entries 9–12). However, the trend of oxidation yields remained stable when the amount of catalyst was further increased to 40 mg (Table 1, entry 12). The impact of reaction temperature on the rate of oxidation reactions was investigated for the model reaction in the presence of a catalyst. The experiment involved varying the temperature from room temperature to 80 °C and analyzing the resulting product yields. The reaction was carried out under optimized conditions for two hours. The results, as shown in Table 1, indicate that the yield of the product gradually increased as the reaction temperature was raised. At room temperature, the reaction rate was relatively low, suggesting that the reaction was not proceeding efficiently under these conditions. As the temperature was increased to 40 °C, the yield improved to a moderate level, indicating a faster rate of reaction. The highest yield of the product was obtained at 60 °C, where the reaction rate was optimized. This temperature provided the most favorable conditions for the oxidation reaction to occur, resulting in a high yield of the desired product. However, when the temperature was further increased to 80 °C, the yield showed a slight decrease compared to 60 °C, indicating that the reaction might have started to deviate from the optimal conditions (Table 1, entries 13–15).

The scope and generality of the oxidation reaction using aldehydes were investigated under the optimized conditions. The results are summarized in Table 2, showing the yields of benzoic acid derivatives obtained from

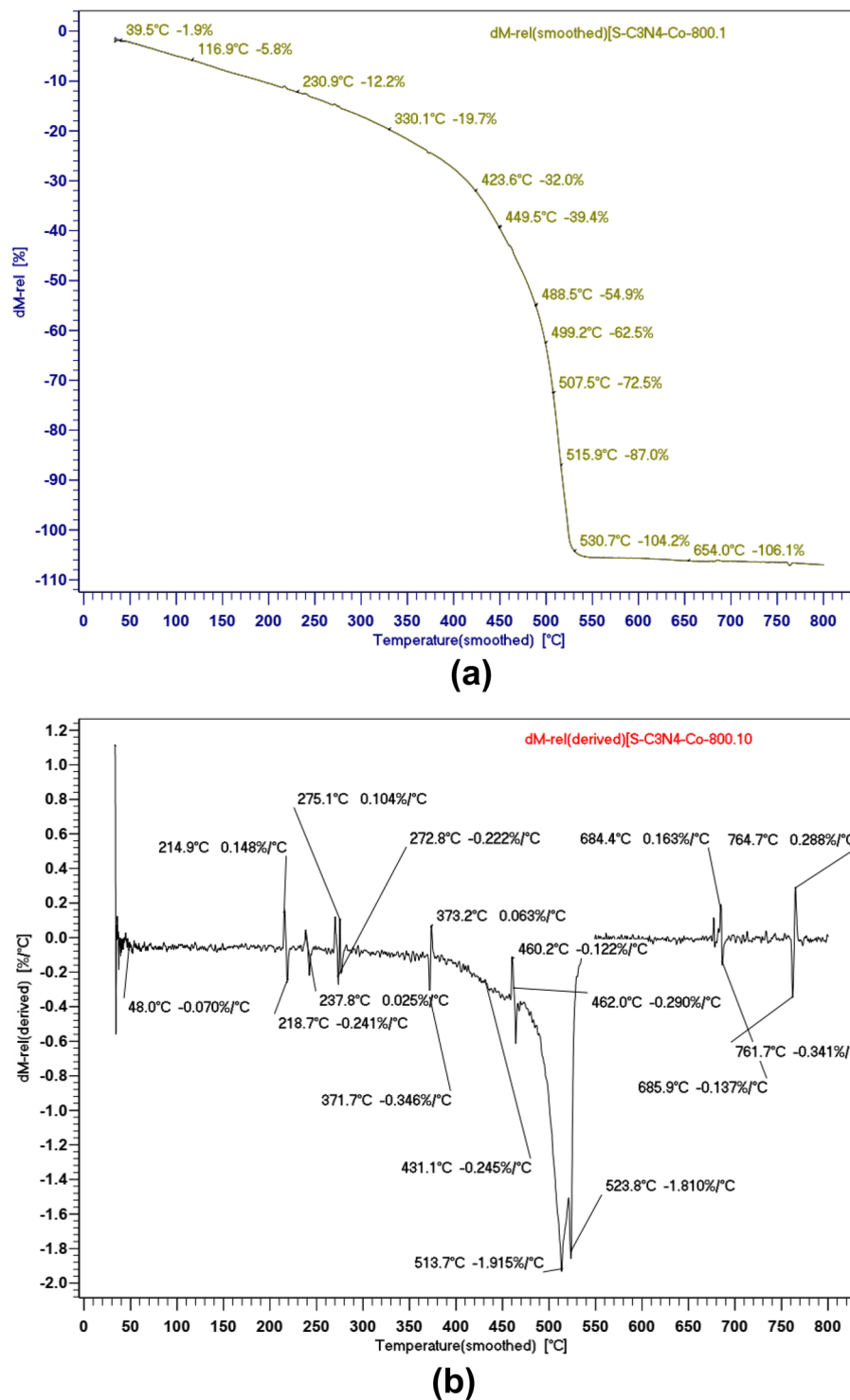



Figure 6. (a) TGA curve Co(salen)@g-C₃N₄. (b) TG curve Co(salen)@g-C₃N₄.

various aldehyde derivatives. The oxidation of different aromatic and heteroaromatic aldehydes to benzoic acid derivatives was successful, with good to excellent yields. The electronic properties and steric effects of substituents on the aromatic aldehydes did not significantly influence the reaction, as the yields remained consistently high across different substituents. Aromatic aldehydes bearing both electron-withdrawing and electron-donating groups gave well to excellent yields, indicating the versatility of the reaction. Even heteroaromatic aldehydes reacted smoothly, yielding excellent results. Aldehydes containing electron-donating groups like OCH₃ and CH₃, provided moderate yields. The oxidation reactions were carried out at 60 °C and typically reached completion within a few hours (2–5 h). The isolated yields of the benzoic acid products were generally quantitative, indicating the efficiency of the optimized reaction conditions.



Entry	M(salen)@g-C ₃ N ₄ (mg)	Amount of H ₂ O ₂ (mmol)	Time (h)	Temp (°C)	Yield (%) ^a
1	–	3	20	25	30
2	Mn(salen)@g-C ₃ N ₄ (30 mg)	3	20	25	62
3	Cu(salen)@g-C ₃ N ₄ (30 mg)	3	20	25	58
4	Co(salen)@g-C ₃ N ₄ (30 mg)	3	20	25	98
5	Co(salen)@g-C ₃ N ₄ (30 mg)	2.5	20	25	89
6	Co(salen)@g-C ₃ N ₄ (30 mg)	2	20	25	78
7	Co(salen)@g-C ₃ N ₄ (30 mg)	1.5	20	25	76
8	Co(salen)@g-C ₃ N ₄ (30 mg)	1.0	20	25	62
9	Co(salen)@g-C ₃ N ₄ (5 mg)	3	20	25	51
10	Co(salen)@g-C ₃ N ₄ (10 mg)	3	20	25	68
11	Co(salen)@g-C ₃ N ₄ (20 mg)	3	20	25	81
12	Co(salen)@g-C ₃ N ₄ (40 mg)	3	20	25	98
13	Co(salen)@g-C ₃ N ₄ (30 mg)	3	8	40	65
14 ^b	Co(salen)@g-C ₃ N ₄ (30 mg)	3	2	60	98 (98,98, 98) ^b
15	Co(salen)@g-C ₃ N ₄ (30 mg)	5	2	80	98

Table 1. Optimization of reaction parameter on the model reaction. ^aGC yields ^bThe reaction was repeated for three times.

The scalability of the oxidation method was evaluated by conducting a gram-scale oxidation of benzaldehyde using the optimized conditions. Remarkably, the oxidation of benzaldehyde on a 10 g scale, with a catalyst amount of only 200 mg, resulted in an impressive isolated yield of 98% for the desired benzoic acid product. This gram-scale oxidation demonstrates the practical applicability of the method and its potential for large-scale synthesis. The use of a relatively small amount of catalyst in proportion to the reaction scale further highlights the efficiency and cost-effectiveness of the process.

The reusability of the carbon nitride-based catalyst was investigated in a model reaction with a 5 mmol-scale reaction using 100 mg of catalyst. The results are summarized in Fig. 7, showing the performance of the recovered catalyst in successive runs. In the first and second runs (Fig. 7, entries 1 and 2), the recovered catalyst exhibited excellent reusability, maintaining its efficiency with high product yields. This indicates the stability and robustness of the catalyst, allowing for multiple reaction cycles without significant loss in performance. However, in the third and fourth runs (Fig. 7, entries 3 and 4), a slight decrease in product yield was observed. Overall, the carbon nitride catalyst showed good reusability up to the five-run, with high product yields.

A comparison was made between the prepared Co(salen)@g-C₃N₄ catalysts for the oxidation of benzaldehyde to benzoic acid with other reported procedures. The comparison highlighted the advantages of the proposed methodology in terms of reaction times, yields, and the environmentally friendly nature of the process. The results in Table 3 demonstrate that the Co(salen)@g-C₃N₄ catalysts exhibit shorter reaction times, excellent yields, and importantly, offer a greener alternative compared to other methodologies^{58–64}.

Based on the available data and previous reports⁶⁴, a mechanistic proposal for the oxidation of aldehyde to acid catalyzed by cobalt can be outlined (Fig. 8). In this proposed mechanism, cobalt acts as a catalyst to facilitate the reaction. Initially, the cobalt catalyst undergoes coordination and activation of aldehyde and H₂O₂. H₂O₂ acting as a nucleophile, adds to the activated aldehyde with the assistance of the cobalt catalyst, and carbon nitride facilitated the abstraction of hydrogen from H₂O₂ and the formation of water. It is worth noting that a radical mechanism may also be involved in cobalt-catalyzed reactions, although further investigation is required to elucidate the precise details⁶⁴.

Conclusion

In this study, a novel series of reusable M(salen)@g-C₃N₄ catalysts (M=Co, Cu, Mn) was synthesized by incorporating metal complexes (salen) onto the g-C₃N₄ host. These catalysts exhibited exceptional performance for the oxidation of aldehyde derivatives in the presence of H₂O₂ at mild reaction conditions with short reaction times. Among them, the Co(salen)@g-C₃N₄ catalyst demonstrated the best catalytic activity and was further optimized for oxidation conditions. The catalysts displayed high efficiency, durability, and recyclability, making them suitable for long-term operations. The method also proved to be robust and reliable, providing a valuable approach for synthesizing benzoic acid derivatives on a larger scale. Moreover, the scalability of the method was demonstrated by achieving high isolated yields on a gram scale, indicating its robustness and reliability for synthesizing larger quantities of benzoic acid derivatives.

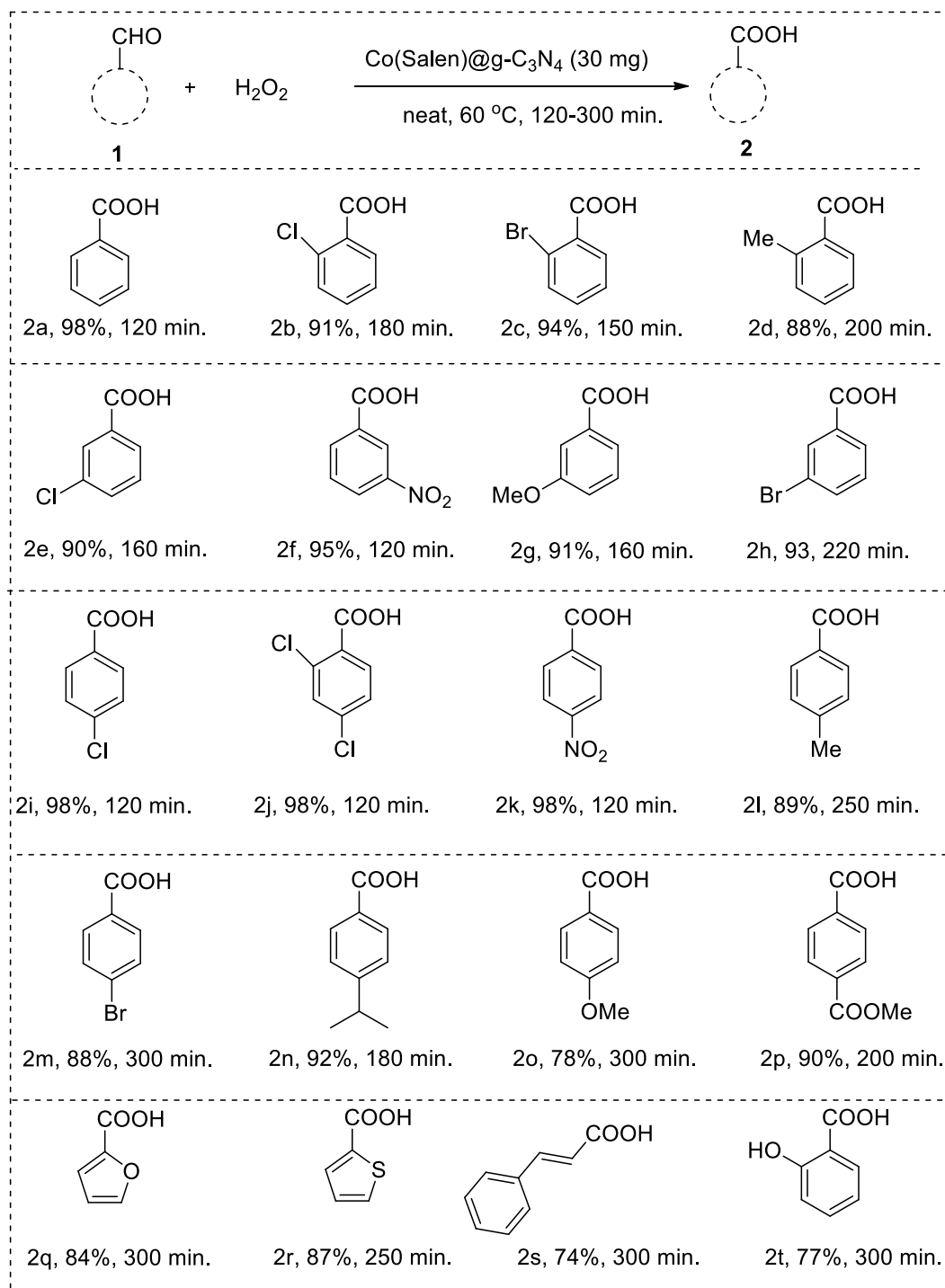


Table 2. Scope and generality of the oxidation reaction using aldehydes.

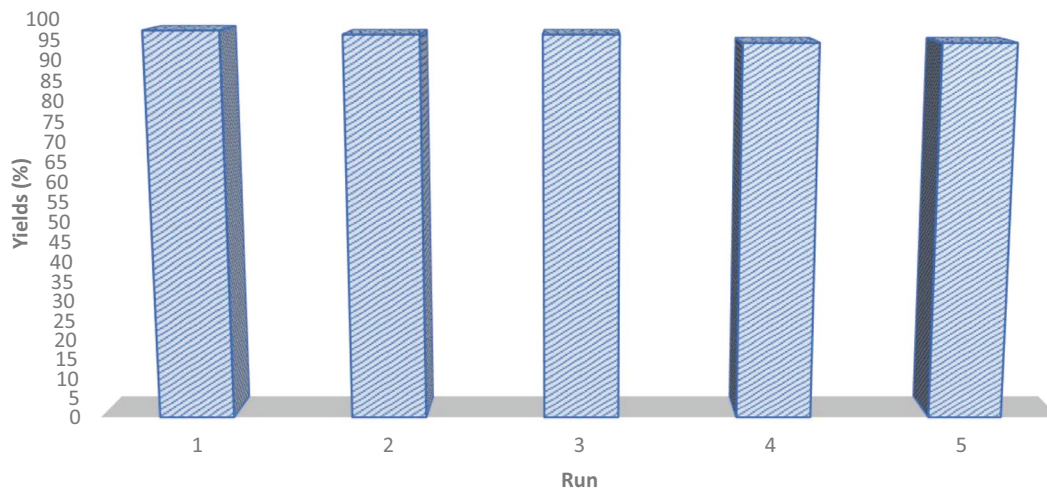


Figure 7. Reusability of the carbon nitride catalyst in a mole-scale reaction.

Entry	Reaction condition	Solvent	Temp (°C)	Time (h)	Yield (%)	References
a	H ₃ PW ₁₂ O ₄₀ , Al-MCM-48, H ₂ O ₂	Neat	80	6	81	⁵⁸
b	[MoO ₃ (trz) _{0.5}], H ₂ O ₂	Water	70	24	80	⁵⁹
c	MOF-Zn-NHC, Et ₃ N, O ₂	Water	100	3.5	80	⁶⁰
d	AuNPs/BPy-PMO, NaHCO ₃ , O ₂	Water	30	2	87	⁶¹
e	KBrO ₃ /KBr, HCl	Water	100	3	50	⁶²
f	Oxone	DMF	rt	3	97	³⁸
g	Ni(OAc) ₂ , O ₂ , 6205 Torr	Ethanol/Water	20	0.5	80	⁵³
h	Whole-cell biocatalyst	KPi	35	12	99	⁴⁰
i	Geopolymer supported CuO	Neat	80	10	67	⁶³
j	hydroxycyclohexylphenylketon	NaOH/DME	80	3	99	⁴²
k	Co(salen)@g-C ₃ N ₄ , H ₂ O ₂	Neat	60	2	98	This work

Table 3. Comparison of literature for oxidation of benzaldehyde.

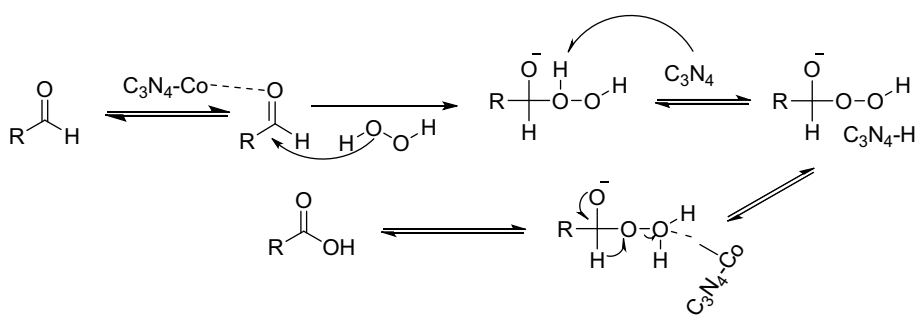


Figure 8. Proposed mechanism.

Data availability

The data that support the findings of this study are available on request from the corresponding author.

Received: 25 December 2023; Accepted: 4 April 2024

Published online: 11 April 2024

References

- Dess, D. B. & Martin, J. C. A useful 12-1-5 triacetoxyperiodinane (the Dess-Martin Periodinane) for the selective oxidation of primary or secondary alcohols and a variety of related 12-i-5 species. *J. Am. Chem. Soc.* **113**(19), 7277–7287 (1991).
- Anelli, P. L., Biffi, C., Montanari, F. & Quici, S. Fast and selective oxidation of primary alcohols to aldehydes or to carboxylic acids and of secondary alcohols to ketones mediated by oxoammonium salts under two-phase conditions. *J. Org. Chem.* **52**(12), 2559–2562 (1987).
- Corey, E. J., Gilman, N. W. & Ganem, B. E. New methods for the oxidation of aldehydes to carboxylic acids and esters. *J. Am. Chem. Soc.* **90**(20), 5616–5617 (1968).
- Travis, B. R., Sivakumar, M., Hollist, G. O. & Borhan, B. Facile oxidation of aldehydes to acids and esters with Oxone. *Org. Lett.* **5**(7), 1031–1034 (2003).
- Müller, P. & Godoy, J. Catalyzed oxidation of alcohols and aldehydes with iodosylbenzene. *Tetrahedron Lett.* **22**(25), 2361–2364 (1981).
- Lin, J.-C., Yi, Y., Zhang, L., Ji, X.-J. & Zhang, Z.-G. A solvent-tolerant whole-cell biocatalyst for chemoselective oxidation of aldehydes to carboxylic acids. *Mol. Catal.* **550**, 113576 (2023).
- Dalcanale, E. & Montanari, F. (1986) Selective oxidation of aldehydes to carboxylic acids with sodium chlorite-hydrogen peroxide. *J. Org. Chem.* **51**(4), 567–569 (1986).
- Lu, Y., Tan, W.-Y., Ding, Y., Chen, W. & Zhang, H. Oxidation of primary alcohols and aldehydes to carboxylic acids with 1-hydroxy-cyclohexyl phenyl ketone. *J. Org. Chem.* **88**(13), 8114–8122 (2023).
- Zarnegaryan, A. Facile synthesis of polyoxometalate supported on magnetic graphene oxide as a hybrid catalyst for efficient oxidation of aldehydes. *Sci. Rep.* **12**(1), 18491 (2022).
- Batsika, C. S., Koutsilieris, C., Koutoulogenis, G. S., Kokotos, C. G. & Kokotos, G. Light-promoted oxidation of aldehydes to carboxylic acids under aerobic and photocatalyst-free conditions. *Green Chem.* **24**(16), 6224–6231 (2022).
- Shi, H., Li, J., Wang, T., Rudolph, M. & Hashmi, A. S. K. Catalyst- and additive-free sunlight-induced autoxidation of aldehydes to carboxylic acids. *Green Chem.* **24**(15), 5835–5841 (2022).
- Woo, J., Moon, B. C., Lee, U., Min, B. K. & Lee, D. K. Collaborative electrochemical oxidation of the alcohol and aldehyde groups of 5-hydroxymethylfurfural by NiOOH and Cu(OH)₂ for superior 2,5-furandicarboxylic acid production. *ACS Catal.* **12**(7), 4078–4091 (2022).
- Tan, W.-Y., Lu, Y., Zhao, J.-F., Chen, W. & Zhang, H. Oxidation of primary alcohols and aldehydes to carboxylic acids via hydrogen atom transfer. *Org. Lett.* **23**(17), 6648–6653 (2021).
- Cheng, A.-D., Zong, M.-H., Lu, G.-H. & Li, N. Solvent-promoted oxidation of aromatic alcohols/aldehydes to carboxylic acids by a laccase-TEMPO system: Efficient access to 2,5-furandicarboxylic acid and 5-methyl-2-pyrazinecarboxylic acid. *Adv. Sustain. Syst.* **5**(6), 2000297 (2021).
- Xu, J., Yue, X., He, L., Liang, C. & Li, W. Photoinduced protocol for aerobic oxidation of aldehydes to carboxylic acids under mild conditions. *ACS Sustain. Chem. Eng.* **10**(43), 14119–14125 (2022).
- Liu, K.-J., Fu, Y.-L., Xie, L.-Y., Xu, X. & He, W.-M. Green and efficient: Oxidation of aldehydes to carboxylic acids and acid anhydrides with air. *ACS Sustain. Chem. Eng.* **6**(4), 4916–4921 (2018).
- Dai, P.-F., Qu, J.-P. & Kang, Y.-B. Organocatalyzed aerobic oxidation of aldehydes to acids. *Org. Lett.* **21**(5), 1393–1396 (2016).
- Yu, H., Ru, S., Zhai, Y., Han, S. & Wei, Y. An efficient aerobic oxidation protocol of aldehydes to carboxylic acids in water catalyzed by an inorganic-ligand-supported copper catalyst. *ChemCatChem* **10**(6), 1253–1257 (2018).
- Yan, X., Lai, Y.-H. & Zare, R. N. Preparative microdroplet synthesis of carboxylic acids from aerobic oxidation of aldehydes. *Chem. Sci.* **9**(23), 5207–5211 (2018).
- Tayyab, M. *et al.* Simultaneous hydrogen production with the selective oxidation of benzyl alcohol to benzaldehyde by a noble-metal-free photocatalyst VC/CdS nanowires. *Chin. J. Catal.* **43**, 1165–1175 (2022).
- Raczuk, E., Dmochowska, B., Samaszko-Fierstek, J. & Madaj, J. Different Schiff bases—Structure, importance and classification. *Molecules* **27**(3), 787 (2022).
- Boulechfar, C. *et al.* Schiff bases and their metal complexes: A review on the history, synthesis, and applications. *Inorg. Chem. Commun.* **150**, 110451 (2023).
- Aggarwal, N. & Maji, S. Potential applicability of Schiff bases and their metal complexes during COVID-19 pandemic: A review. *Rev. Inorg. Chem.* **42**(4), 363–383 (2022).
- Khan, E., Hanif, M. & Akhtar, M. S. Schiff bases and their metal complexes with biologically compatible metal ions: Biological importance, recent trends and future hopes. *Rev. Inorg. Chem.* **42**(4), 307–325 (2022).
- Kumari, S., Seema, Yadav, P., Sharma, S. & Ranka, M. Amino acid based Schiff bases and their metal complexes as biologically potent agents: A review. *Asian J. Chem.* **34**(10), 2465–2477 (2022).
- Nath, B. D., Islam, M. M., Karim, M. R., Georghiou, P. E. & Menelaou, M. Recent progress in metal-incorporated acyclic schiff-base derivatives: Biological aspects. *ChemistrySelect* **7**(14), 202104290 (2022).
- Arunadevi, A. & Raman, N. Biological response of Schiff base metal complexes incorporating amino acids: A short review. *J. Coord. Chem.* **73**(15), 2095–2116 (2020).
- Mahadevi, P. & Sumathi, S. Mini review on the performance of Schiff base and their metal complexes as photosensitizers in dye-sensitized solar cells. *Synth. Commun.* **50**(15), 2237–2249 (2020).
- Uddin, M. N., Ahmed, S. S. & Alam, S. M. R. Review: Biomedical applications of Schiff base metal complexes. *J. Coord. Chem.* **73**(23), 3109–3149 (2020).
- Rao, D. P. A review on versatile applications of novel Schiff bases and their metal complexes. *Lett. Appl. NanoBioScience* **8**(4), 675–681 (2019).
- Berhanu, A. L., Gaurav, Mohiuddin, I., Kumar, V. & Kim, K.-H. A review of the applications of Schiff bases as optical chemical sensors. *TrAC-Trends Anal. Chem.* **116**, 74–91 (2019).
- Tadele, K. T. & Tsega, T. W. Schiff bases and their metal complexes as potential anticancer candidates: A review of recent works. *Anti-Cancer Agents Med. Chem.* **19**(15), 1786–1795 (2019).
- Hameed, A., al-Rashida, M., Uroos, M., Abid Ali, S. & Khan, K. M. Schiff bases in medicinal chemistry: A patent review (2010–2015). *Expert Opin. Therapeut. Patents* **27**(1), 63–79 (2017).
- Kumar, S., Dhar, D. N. & Saxena, P. N. Applications of metal complexes of Schiff bases: A review. *J. Sci. Ind. Res.* **68**(3), 181–187 (2009).
- Liu, X., Manzur, C., Novoa, N., Carrillo, D. & Hamon, J.-R. Multidentate unsymmetrically-substituted Schiff bases and their metal complexes: Synthesis, functional materials properties, and applications to catalysis. *Coord. Chem. Rev.* **357**, 144–172 (2018).

36. Wang, X. *et al.* A metal-free polymeric photocatalyst for hydrogen production from water under visible light. *Nat. Mater.* **8**(1), 76–80 (2009).
37. Wang, X. C. *et al.* Polymer semiconductors for artificial photosynthesis: Hydrogen evolution by mesoporous graphitic carbon nitride with visible light. *J. Am. Chem. Soc.* **131**(44), 1680–1681 (2009).
38. Zhang, G., Zhang, J., Zhang, M. & Wang, X. Polycondensation of thiourea into carbon nitride semiconductors as visible light photocatalysts. *J. Mater. Chem.* **22**, 8083–8091 (2012).
39. Wang, Y., Wang, X. & Antonietti, M. Polymeric graphitic carbon nitride as a heterogeneous organocatalyst: From photochemistry to multipurpose catalysis to sustainable chemistry. *Angewandte Chemie-Int. Edition* **51**(1), 68–89 (2012).
40. Wang, X., Blechert, S. & Antonietti, M. Polymeric graphitic carbon nitride for heterogeneous photocatalysis. *ACS Catal.* **2**(8), 1596–1606 (2012).
41. Zhao, Z., Sun, Y. & Dong, F. Graphitic carbon nitride based nanocomposites: A review. *Nanoscale* **7**(1), 15–37 (2015).
42. Zhu, J., Xiao, P., Li, H. & Carabineiro, S. A. C. Graphitic carbon nitride: Synthesis, properties, and applications in catalysis. *ACS Appl. Mater. Interfaces* **6**(19), 16449–16465 (2014).
43. Liu, J., Wang, H. & Antonietti, M. Graphitic carbon nitride reloaded: Emerging applications beyond (photo)catalysis. *Chem. Soc. Rev.* **45**(8), 2308–2326 (2016).
44. Tayyab, M. *et al.* A new breakthrough in photocatalytic hydrogen evolution by amorphous and chalcogenide enriched cocatalysts. *Chem. Eng. J.* **455**, 140601 (2023).
45. Masih, D., Ma, Y. & Rohani, S. Graphitic C₃N₄ based noble-metal-free photocatalyst systems: A review. *Appl. Catal. B Environ.* **206**, 556–588 (2017).
46. Liu, H. *et al.* Linking melem with conjugated Schiff-base bonds to boost photocatalytic efficiency of carbon nitride for overall water splitting. *Nanoscale* **13**, 9315–9321 (2021).
47. Fina, F., Callear, S. K., Carins, G. M. & Irvine, J. T. S. Structural investigation of graphitic carbon nitride via XRD and neutron diffraction. *Chem. Mater.* **27**(7), 2612–2618 (2015).
48. Liu, Y. *et al.* Single-atom Pt loaded zinc vacancies ZnO–ZnS induced type-V electron transport for efficiency photocatalytic H₂ evolution. *Solar RRL* **5**, 2100536 (2021).
49. Das, S., Deka, T., Ningthoukhangjam, P., Chowdhury, A. & Nair, R. G. A critical review on prospects and challenges of metal-oxide embedded g-C₃N₄-based direct Z-scheme photocatalysts for water splitting and environmental remediation. *Appl. Surface Sci. Adv.* **11**, 100273 (2022).
50. Thomas, S. A., Pallavolu, M. R., Khan, M. E. & Cherusseri, J. Graphitic carbon nitride (g-C₃N₄): Futuristic material for rechargeable batteries. *J. Energy Storage* **68**, 107673 (2023).
51. Ong, W.-J., Tan, L.-L., Ng, Y. H., Yong, S.-T. & Chai, S.-P. Graphitic carbon nitride (g-C₃N₄)-based photocatalysts for artificial photosynthesis and environmental remediation: Are we a step closer to achieving sustainability?. *Chem. Rev.* **116**(12), 7159–7329 (2016).
52. Tayyab, M. *et al.* One-pot in-situ hydrothermal synthesis of ternary In₂S₃/Nb₂O₅/Nb₂C Schottky/S-scheme integrated heterojunction for efficient photocatalytic hydrogen production. *J. Colloid Interface Sci.* **628**, 500–512 (2022).
53. Yue, W. *et al.* Schottky junction enhanced H₂ evolution for graphitic carbon nitride-NiS composite photocatalysts. *J. Colloid Interface Sci.* **657**, 133–141 (2024).
54. Azizi, N., Farhadi, E. & Farzaneh, F. Increased catalytic activity through ZnMo₇O₂₄/g-C₃N₄ heterostructured assemblies for greener indole condensation reaction at room temperature. *Sci. Rep.* **12**(1), 18634 (2022).
55. Azizi, N. & Edrisi, M. Preparation of choline sulfate ionic liquid supported on porous graphitic carbon nitride nanosheets by simple surface modification for enhanced catalytic properties. *J. Mol. Liquids* **300**, 112263 (2020).
56. Mirmashhori, B., Azizi, N. & Saidi, M. R. A simple, economical, and highly efficient synthesis of β-hydroxynitriles from epoxide under solvent free conditions. *J. Mol. Catal. A Chem.* **247**(1–2), 159–161 (2006).
57. Meng, J. *et al.* Assembling of Al-MCM-48 supported H₃PW₁₂O₄₀ mesoporous materials and their catalytic performances in the green synthesis of benzoic acid. *Mater. Res. Bull.* **60**, 20–27 (2014).
58. Amarante, T. R. *et al.* Metal oxide-triazole hybrids as heterogeneous or reaction-induced self-separating catalysts. *J. Catal.* **340**, 354–367 (2016).
59. Babaei, S., Zarei, M. & Zolfigol, M. A. MOF-Zn-NHC as an efficient N-heterocyclic carbene catalyst for aerobic oxidation of aldehydes to their corresponding carboxylic acids via a cooperative geminal anomeric based oxidation. *RSC Adv.* **11**, 36230–36236 (2021).
60. Ishito, N., Nakajima, K., Maegawa, Y., Inagaki, S. & Fukuoka, A. Facile formation of gold nanoparticles on periodic mesoporous bipyridine-silica. *Catal. Today* **298**, 258–262 (2017).
61. Sharma, G. V. R. & Robert, A. R. Oxidation of aromatic aldehydes with potassium bromate–bromide reagent and an acidic catalyst. *Res. Chem. Intermed.* **39**, 3251–3254 (2013).
62. Upadhyay, J., Misra, S. P., Irusta, S. & Sharma, S. Oxidation of aldehydes to carboxylic acids over geopolymer supported CuO. *Mol. Catal.* **536**, 112911 (2023).
63. Tayyab, M. *et al.* Visible light-driven photocatalytic H₂ evolution and dye degradation by electrostatic self-assembly of CdS nanowires on Nb₂C MXene. *Int. J. Hydrogen Energy* **51**, 1400–1413 (2024).
64. Watanabe, I., Kaiho, A., Kusama, H. & Iwasawa, N. Cobalt-salen complex-catalyzed oxidative generation of alkyl radicals from aldehydes for the preparation of hydroperoxides. *J. Am. Chem. Soc.* **135**(32), 11744–11747 (2013).

Author contributions

All authors contributed to the study's conception and design. R.E. performed material preparation, data collection and analysis. The first draft of the manuscript was written by N.A., and M.B. supervised and Writing–review and editing. All authors read and approved the final manuscript.

Funding

The authors declare that no funds, grants, or other support were received during the preparation of this manuscript.

Competing interests

The authors declare no competing interests.

Additional information

Supplementary Information The online version contains supplementary material available at <https://doi.org/10.1038/s41598-024-58946-3>.

Correspondence and requests for materials should be addressed to M.B. or N.A.

Reprints and permissions information is available at www.nature.com/reprints.

Publisher's note Springer Nature remains neutral with regard to jurisdictional claims in published maps and institutional affiliations.



Open Access This article is licensed under a Creative Commons Attribution 4.0 International License, which permits use, sharing, adaptation, distribution and reproduction in any medium or format, as long as you give appropriate credit to the original author(s) and the source, provide a link to the Creative Commons licence, and indicate if changes were made. The images or other third party material in this article are included in the article's Creative Commons licence, unless indicated otherwise in a credit line to the material. If material is not included in the article's Creative Commons licence and your intended use is not permitted by statutory regulation or exceeds the permitted use, you will need to obtain permission directly from the copyright holder. To view a copy of this licence, visit <http://creativecommons.org/licenses/by/4.0/>.

© The Author(s) 2024